


## Article

# Monitoring and Investigating the Change Patterns of Major Growth Parameters of Almond (Badam) Trees under Different Irrigation Conditions

Huimin Yang<sup>1,2</sup>, Yunlong San<sup>3</sup>, Yifei Chen<sup>1</sup>, Yan Ma<sup>1</sup>, Xuenong Wang<sup>1</sup>, Muhammad Rizwan Shoukat<sup>4</sup> ,  
Yudong Zheng<sup>4,\*</sup> and Xin Hui<sup>4,\*</sup>

- <sup>1</sup> Agricultural Mechanization Institute, Xinjiang Academy of Agricultural Sciences, Urumqi 830091, China; yhm\_shz@163.com (H.Y.); cyfgunman@163.com (Y.C.); 1910751102@mail.sit.edu.cn (Y.M.); xjwxn2010@sina.com (X.W.)
- <sup>2</sup> Scientific Observation and Experimental Station of Forest Fruit and Cotton Equipment, Ministry of Agriculture and Rural Affairs, Urumqi 830091, China
- <sup>3</sup> School of Mechanical Engineering, Hubei Engineering University, Xiaogan 432000, China; sanyunlong@163.com
- <sup>4</sup> College of Water Conservancy and Civil Engineering, China Agricultural University, Beijing 100193, China; rizwan3147@gmail.com
- \* Correspondence: 15612771262@163.com (Y.Z.); xin0821h@163.com (X.H.)

**Abstract:** Knowledge of the response of growth parameters of almond (Badam) trees to different water supply conditions is important for Badam production. To identify growth parameters that are sensitive to water deficit in almond trees, field experiments were conducted during a median water year to monitor the major growth characteristics of almond trees under different irrigation conditions in Shache County, Xinjiang, China. A field (in-situ) monitoring system was also constructed using various sensors for the continuous and non-destructive monitoring of the growth parameters, such as soil water in the root zone, canopy temperature depression, trunk diameter, and fruit diameter of almond trees. The results confirmed the reliability of the monitoring system. Both canopy temperature depression and the diameter shrinkage of the trunk and fruit were significantly negatively correlated ( $r$  values ranging from  $-0.996$  to  $-0.823$ ) with the irrigation water quantity. This correlation was observed from the young fruit stage to the maturation stage of almond trees, under irrigation conditions representing 50–100% of crop evapotranspiration (ET<sub>c</sub>). These parameters were sensitive ( $|r| \geq 0.778$ ) to the water deficit status of almond trees from 14:00 to 18:00 in sunny weather. These results can provide both technical and theoretical support for real-time non-destructive assessment of the water deficit status of almond trees.



**Citation:** Yang, H.; San, Y.; Chen, Y.; Ma, Y.; Wang, X.; Shoukat, M.R.; Zheng, Y.; Hui, X. Monitoring and Investigating the Change Patterns of Major Growth Parameters of Almond (Badam) Trees under Different Irrigation Conditions. *Water* **2023**, *15*, 3731. <https://doi.org/10.3390/w15213731>

Academic Editors: Shouzheng Jiang and Jing Zheng

Received: 26 August 2023

Revised: 8 October 2023

Accepted: 18 October 2023

Published: 26 October 2023



**Copyright:** © 2023 by the authors. Licensee MDPI, Basel, Switzerland. This article is an open access article distributed under the terms and conditions of the Creative Commons Attribution (CC BY) license (<https://creativecommons.org/licenses/by/4.0/>).

**Keywords:** almond (Badam); irrigation conditions; soil moisture; canopy temperature; trunk diameter; fruit diameter

## 1. Introduction

Almonds (Badam) are one of the most popular dried fruits in the world [1]. The promotion and planting of almond trees have played a very important role in enhancing regional GDP and building ecological barriers [2]. Xinjiang is the main production area of almonds in China, of which the planting area in Shache County alone has reached approximately 60,213 ha, with a total output of approximately 93,000 tons. Reduced fruit yield, plant height, leaf area, and stomatal conductance are the result of water stress, which has a substantial impact on the growth and physiological features of almond trees [3–5]. According to Hang et al. [6], fruit trees receiving deficit irrigation grow less than those receiving reasonable irrigation and the scarcity of water resources in the main planting areas of Xinjiang should be considered [7]. These results underline the importance of understanding how water shortages affect almond farming and the necessity of efficient

water management measures to promote optimum development and nutrient uptake in places like Shache County, Xinjiang.

Water deficit limits transpiration and the dissipation of the associated latent heat of evaporation [8], and lead to changes in plant growth parameters such as leaf temperature [9], trunk [10], and fruit volume [11]. Plant water potential is an important indicator to assess crop water stress. But the use of the leaf pressure chamber is complicated, and it requires a relatively long time for manual measurement. Continuous monitoring of fruit tree growth dynamics using relatively simple, reliable, and nondestructive sensors allows researchers to assess water supply status in a timely manner [12,13]. Since the temperature of the leaves rises in the early stages of water stress, the tree's response to drought can be monitored using thermal sensors mounted above the canopy [6]. In addition, the diameter of the trunk or fruit fluctuates depending on the water content of the tissues [14–16]. Therefore, the use of diameter measuring instruments can effectively identify the water supply status of fruit trees. The use of these sensors can better explain the relationship between fruit tree growth patterns and moisture environment.

At present, many scholars have carried out relevant research on the monitoring of water stress in fruit trees. Because leaf temperature rises in the water stress state [17], water stress can be monitored by measuring the canopy temperature of the fruit trees. For example, Gomez-Candon et al. [18] continuously observed the response of different apple varieties to a progressive water deficit environment by placing a thermal radiation sensor 1.50 m above the canopy. In addition, the threshold criteria for drought stress in fruit trees can be constructed using parameters such as canopy thermography [18] or the ratio of canopy temperature to carbon isotopes [19]. Water deficit can lead to volume shrinkage of plant organs (stems, fruits, leaves, etc.); therefore, micro-changes in plant organ volume can be used as diagnostic indicators of water scarcity [20] and guide irrigation [21]. Velez et al. [22], Conejero et al. [23,24], Puerto et al. [25], and Du et al. [26] studied trunk diameter changes and found that the maximum daily trunk shrinkage was relatively reliable when assessing the moisture status of citrus, peach, almond, and apple plants. Monitoring water stress by combining micro-changes in the volume of multiple plant organs [27,28] is also a current research trend. Based on this method, fruit yield evaluation, variety selection, and evapotranspiration prediction can be realized. For example, Mesejo et al. [29] studied the changes in the canopy temperature, trunk diameter, and fruit diameter of citrus trees under different soil and water conditions and concluded that variations in the water status increased the probability of fruit cracking. Ruas et al. [30] investigated the differences in the chlorophyll content and leaf area of two different varieties of papaya under different irrigation conditions and completed the screening of drought-resistant papaya genotypes. Zambrano-Vaca et al. [31] found that the canopy cover area and trunk cross-sectional area of peach seedlings correlate significantly with plant water consumption and can be used to further estimate actual daily evapotranspiration. Although the above research is rich and diverse, there are few studies on the water stress of almond (Badam) trees in Xinjiang.

Therefore, this study aimed to examine the changes in the major growth parameters of almond trees in relation to water supply conditions through field experiments based on the constructed measurement system in Xinjiang. The specific research objectives of this study were as follows: (1) to use various sensors to construct a monitoring system that can continuously and non-destructively measure the growth environment and physiological data of almond trees; (2) to perform an irrigation experiment covering all the growth stages of almond trees under different irrigation levels, and summarize the changing patterns of various physiological parameters related to almond trees under different SWCs; and (3) to select physiological parameters and measuring time during the day in Xinjiang that can be useful for monitoring the water deficit status of almond (Badam) trees based on the changing patterns of various physiological parameters. The research roadmap is shown in Figure 1.

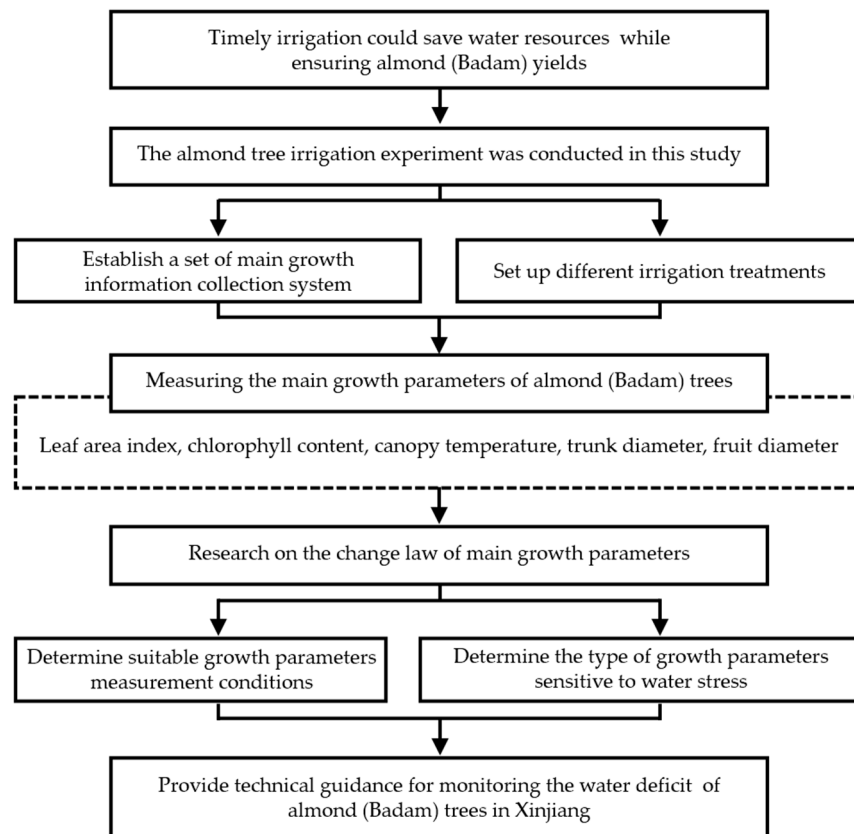


**Figure 1.** Research idea roadmap for this study.

## 2. Materials and Methods

### 2.1. Experimental Site

The experiments were carried out in the state-owned No. 2 Forest Farm in Shache County (Kashgar, Xinjiang, China; latitude:  $38^{\circ}12'1''$  N, longitude:  $77^{\circ}8'20''$  E). This experimental site is located in Aslanbagh Town in the south of Shache County, which is in the northern foothills of the Kunlun Mountains and in the middle and upper reaches of the Yarkant River. The site has a temperate continental climate, which is characterized by four distinct seasons, dry weather, long sunshine hours, large evaporation, more sunny days, and a large temperature difference between day and night. It has an elevation of 1231.2 m and an average annual temperature of  $11.4^{\circ}\text{C}$ . The precipitation varies greatly, and the annual average precipitation ranges from 46.1 to 50.0 mm. Although the precipitation is low, it is concentrated in specific months, mostly from April to September. Northwesterly winds prevail throughout the year, with annual average and maximum wind speeds of 1.9 m/s and 28 m/s, respectively. The average frost-free period is 214 days. The average number of sunshine hours throughout the year is 2806 h, and the total annual solar radiation is  $145.8\text{ kcal/cm}^2$  [7]. The soil type at the experimental site is sandy loam, with the bulk density of  $1.45\text{ g/cm}^3$ , the permanent wilting point is 5.8% ( $v/v$ ), and the field capacity of the soil is 35.19% ( $v/v$ ) within 100 cm, an organic matter content of 10.69 g/kg, quick-release contents of nitrogen 51.55 mg/kg, phosphorus 7.59 mg/kg, and potassium 143.90 mg/kg, and a pH of 8.2 [32]. Surface water was used for irrigation, mainly from the Yarkant River which was approximately 150 m from the experimental site.

The almond (Badam) variety “Wanfeng” (Shache-18) was used for the experiments. Almond trees of this variety were planted with a row spacing of 8 m and a plant spacing of 6 m. The growing environment is shown in Figure 2, and the specific irrigation treatments employed in the experiment are listed in Table 1. Tree growth was observed from April to July in 2020. The growth period was categorized into five stages: bud swelling from

5 March to 3 April, flowering from 4 April to 13 April, young fruit from 14 April to 10 May, fruit expansion from 11 May to 15 June, and maturation from 16 June to 15 July.

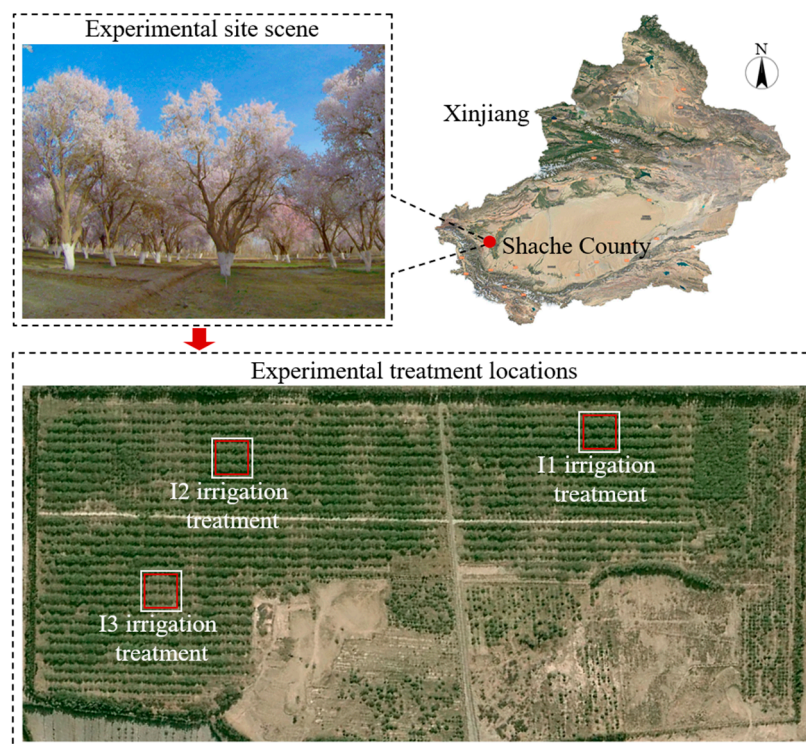


**Figure 2.** Geographic locations of the three irrigation treatments (I1, I2, and I3).

**Table 1.** Irrigation amount (mm) in different irrigation treatments during the critical growth stages of almond trees in 2020.

Irrigation Treatment	Bud Swelling Stage	Flowering Stage	Young Fruit Stage	Fruit Expansion Stage	Maturation Stage
	05/03~03/04	04/04~13/04	14/04~10/05	11/05~15/06	16/06~15/07
I1	90	0	180	270	210
I2	67.5	0	135	202.5	157.5
I3	45	0	90	135	105

## 2.2. Experimental Design

The almond orchard was equipped with a drip irrigation system that included two drip lines for each row of trees. Both were placed 1 m apart from each row. Every tree in the study had twelve drippers (dripper spacing was 0.3 m and the flow rate was 8 L/h), which can create a wetted zone centered on the tree's root with a diameter of approximately 2 m and a wetted depth can be reached of about 1 m. From planting until the irrigation experiments started in 2020 all trees in the orchard received standard commercial dormant pruning and a basal application of 12,000 kg/ha organic fertilizer ( $N + P_2O_5 + K_2O \geq 5.0\%$ ), a follow-up application of 249 kg/ha ammonium sulfate ( $N \geq 21.0\%$ ), 53 kg/ha diammonium phosphate ( $N + P_2O_5 \geq 64.0\%$ ), and 30 kg/ha potassium chloride ( $K_2O \geq 62.0\%$ ) in the spring and were uniformly and adequately irrigated to meet their normal water demands.

The nine-year-old almond trees (medium term of full fruit period) with similar plant height, crown volume, and trunk diameter (with a mean trunk cross-sectional area of  $295 \pm 10 \text{ cm}^2$ ) were selected from the almond orchard to constitute the experimental area. Each irrigation treatment in the experimental area was designed as a randomized complete block. The treatment blocks were spaced approximately 30–50 m apart to prevent

mutual interference between treatments. Each treatment block consisted of 15 trees in three adjacent rows, with the three centrally located almond trees selected as the sample trees for measurement and the remaining trees used as guards. Three irrigation treatments were set up for almond trees: location I1, a full irrigation treatment with an irrigation indicator of 100% crop evapotranspiration ( $ET_c$ ); the other two locations were deficit irrigation treatments, with irrigation indicators of 75%  $ET_c$  (I2) and 50%  $ET_c$  (I3).  $ET_c$  was calculated based on the reference crop evapotranspiration ( $ET_0$ ) and crop coefficient ( $K_c$ ), which can be calculated as follows:

$$ET_c = K_c \times ET_0 \quad (1)$$

where  $ET_c$  is the actual water demand of almond trees in a certain time period (mm/d),  $ET_0$  is the evapotranspiration of local reference crops in a certain time period (mm/d), and it was calculated by the Penman–Monteith method;  $K_c$  is the crop coefficient, which is set with reference to the data provided by the United Nations Food and Agriculture Organization (FAO),  $K_c$  was 0.96, 1.11, 1.29, 1.32, and 0.93 at bud swelling, flowering, young fruit, fruit expansion, and maturation stages, respectively. The amount of water used for irrigation at each growth stage of the tested almond trees is listed in Table 1.

In addition, pest and disease control was performed in the almond orchard according to the growing environment. To ensure 0% weed cover, mowing and herbicide applications were combined to suppress weed growth. All irrigation treatments maintained uniform fertilization management (same as in Section 2.1), which was based on the recommendations in the local almond fertilizer guide.

### 2.3. Collection of Experimental Data

The system for collecting data pertaining to the growth parameters of almond trees during the experiments consisted of a weather station, soil moisture sensor, canopy temperature sensor, plant canopy analyzer, chlorophyll meter, trunk diameter sensor, and fruit diameter sensor. To guarantee the accuracy of the measurement results, all sensors were checked for accuracy before use. This system can collect environmental information such as air temperature, photosynthetically active radiation (PAR), and soil water, as well as plant information such as LAI, chlorophyll content, trunk diameter, and fruit volume, in a real-time manner during the observation period (Figure 3). The time periods for collecting experimental data were the same as those for the growth stages listed in Table 1.

#### 2.3.1. Environmental Meteorological Information

A weather station (ATH-3z, AWL Agricultural Technology (Taizhou) Co., Ltd., Taizhou, China) was set up approximately 2 m above ground to obtain meteorological data such as wind speed, wind direction, PAR (400–700 nm), air temperature, air humidity, and precipitation (Table 2). Based on local 30-year precipitation data, 2020 was a median water year.

#### 2.3.2. Soil Moisture

For each sample tree, a ground location 50–100 cm from the root was selected as the measurement point. Since the root system of the almond tree is predominantly located at a depth of 1 m from the ground surface, soil moisture sensors (SMTE-3z, AWL Agricultural Technology (Taizhou) Co., Ltd., Taizhou, China) were strategically positioned under the drip irrigation belt, near the center of the wetted zone. A vertical alignment was maintained for the sensor probes, which were placed horizontally at distances of 15, 45, and 80 cm from the ground surface. This arrangement was intended to show the soil water content at depths of 0–30 cm, 30–60 cm, and 60–100 cm. To determine the accuracy of the sensors, the oven-drying method was used to verify the data obtained from the soil moisture sensors prior to starting the experiments. Soil moisture content is measured in % ( $v/v$ ).

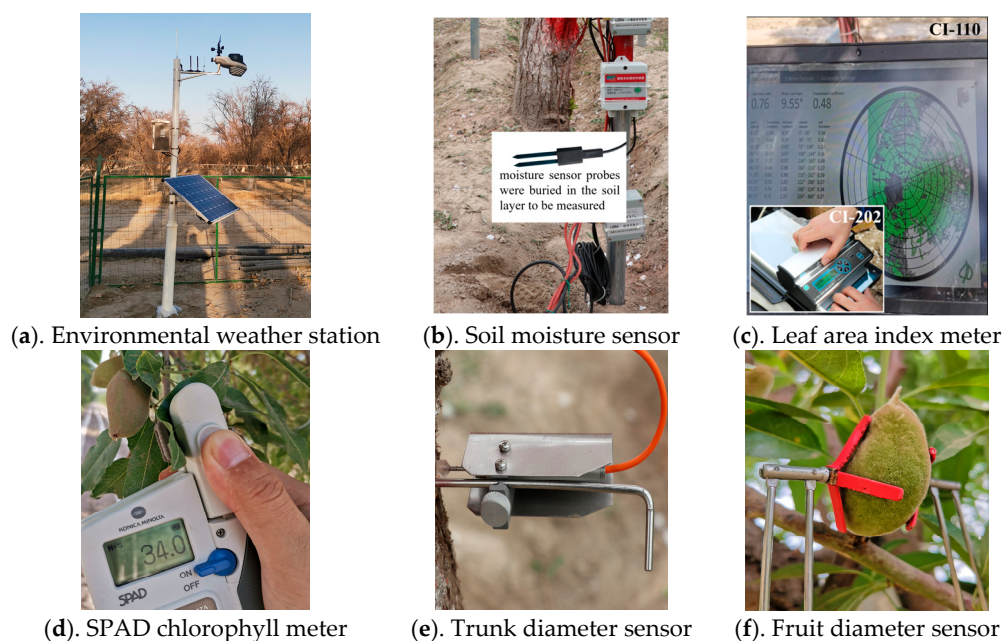


**Figure 3.** Collection of experimental data using different types of sensors; an environmental weather station can acquire the information of both air temperature and photosynthetically active radiation (PAR).

**Table 2.** Environmental meteorological parameters during the experiment in 2020.

Parameter	March	April	May	June	July
Daily mean air temp. (°C)	10.0	16.5	22.5	25.0	26.6
Daily maximum air temp. (°C)	22.8	29.8	35.2	39.7	35.7
Daily minimum air temp. (°C)	−1.3	6.2	10.1	13.9	15.7
Daily minimum relative humidity (%)	30.6	32.7	42.7	36.7	37.4
Daily mean net solar radiation ( $W\ m^{-2}$ )	128	171	256	273	303
Daily mean wind speed ( $m\ s^{-1}$ )	1.71	1.65	1.90	1.89	1.67
Daily mean vapor pressure deficit (kPa)	0.85	1.26	1.55	1.99	2.17
Total precipitation (mm)	3.2	5.1	7.7	9.2	6.6
Reference crop evapotranspiration ( $mm\ day^{-1}$ )	2.9	4.2	4.8	4.7	4.8

### 2.3.3. Canopy Temperature

The canopy temperature was measured using an infrared thermometer (SYS-3205, Liaoning Saiyasi Technology Co., Ltd., Panjin, China), which was employed in this study to measure non-metallic targets using 0.95 emissivity within the 5–14  $\mu m$  wavelength range (infrared). The canopy locations for temperature measurement using the infrared thermometer are shown in Figure 4. At approximately 14:00 every day, three values were measured at approximately 0.5 m above the canopy at each of the four directions (east, south, west, and north) at a 45° angle of elevation back and forth. Their average value was taken as the canopy temperature of the almond trees. In addition, measurements were taken every 2 h from 08:00 to 18:00 in typical weather (sunny and cloudy days) to measure the daily variations in canopy temperature. The canopy/air temperature difference ( $\Delta T$ ) was obtained by calculating the difference between the canopy temperature ( $T_c$ ) and the air temperature ( $T_a$ ) during each measurement.

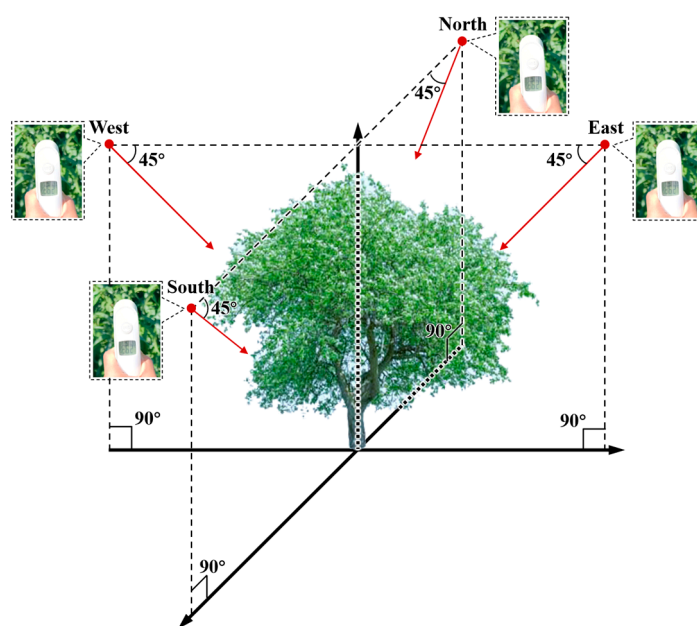


**Figure 4.** Measurements of the canopy temperature from four directions (east, south, west, and north) using an infrared thermometer.

#### 2.3.4. Leaf Area Index

Every three days, we used a plant canopy analyzer (CI-110, CID Inc., Saint Paul, MI, USA) to capture all-sky images of the canopy of the orchard population in clear and windless mornings or evenings (ground observation points were selected every 4.0 m along both the plant spacing and row spacing directions). The software (CI-110 Plant Canopy Imager.1.0) dedicated to the canopy analyzer (CID Inc., Camas, WA, USA) was used to obtain the leaf area index (LAI) data of test trees from the images.

#### 2.3.5. Relative Chlorophyll Content

Six healthy, intact leaves (24 leaves per tree) were labeled in the upper middle (1.5–1.8 m above the ground) of each sample tree from the east, south, west, and north to obtain chlorophyll and leaf area information. A chlorophyll meter (SPAD-502) was used to measure the soil and plant analyzer development (SPAD) values of labeled leaves.

#### 2.3.6. Trunk Diameter

A trunk diameter sensor (SD-6z, AWL Agricultural Technology (Taizhou) Co., Ltd., China, with an accuracy of 0.002 mm) was installed 20 cm above the ground at the bottom of the trunk of each sample tree to measure trunk diameter shrinkage (TDS). The trunk diameter sensor monitored the data every 10 min.

#### 2.3.7. Fruit Diameter

One healthy almond fruit with uniform growth was selected near the labeled leaves (from four directions: east, south, west, and north) as the sample fruit for measurement (a total of four fruits were measured per tree). Then a fruit diameter sensor (FI-Sz, AWL Agricultural Technology (Taizhou) Co., Ltd., Taizhou, China, with an accuracy of 0.02 mm) was used to measure the fruit diameter shrinkage (FDS).

#### 2.3.8. Yield

Fruits of the observed plants were harvested during the maturation stage. After each harvest, fresh fruit was weighed using an electronic scale (1.0 g). The flesh was then stripped from the kernel and sun-dried until the kernel was dry and brittle (with a water content of 8%). The nut yields were calculated separately for kernel with and without flesh.

Finally, the average yield per plant for each irrigation treatment was calculated based on the yield data.

#### 2.4. Data Analysis

Origin 2019b (OriginLab, Northampton, MA, USA) was used to present the scatter plots, point-line plots, and correlation heat maps of the experimentally observed parameters. The correlations (Pearson's correlation coefficient  $r$ ) between the parameters and the significance of these correlations were evaluated using the analysis of variance (ANOVA) using SPSS 20.0 (IBM Corp., Armonk, NY, USA).

### 3. Results and Analysis

#### 3.1. Variations of Measured Indicator Parameters

After completing sensor installation and accuracy verification, the data for the target parameters were monitored. The parameters measured in the experiment were categorized into two types: crop and environmental. The crop parameters included  $\Delta T$ , LAI, chlorophyll content, and fruit and trunk diameter variation. In addition to the SWC, the environmental parameters also included PAR values to better understand the change patterns of crop parameters [27,30,33].

##### 3.1.1. Soil Water Content

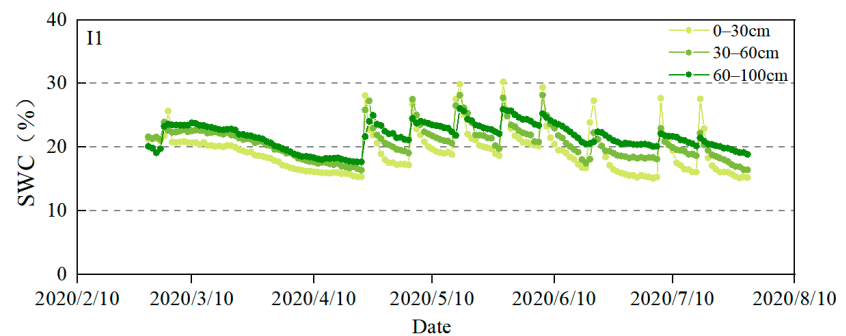
The variations of soil water content (SWC) under different irrigation treatments are shown in Figure 5. The overall SWC under I1 treatment was the highest (Figure 5a), ranging from 15.10 to 30.28%. This was followed by the I2 treatment (Figure 5b), with the overall SWC ranging from 13.19 to 28.18%. The lowest SWC throughout the growth stages was observed in I3 treatment (Figure 5c), ranging from 9.90 to 25.54%. As shown in Figure 5, SWC exhibited a peak of significant increase at each critical growth stage when irrigation was performed (3 March 2020, 23 April 2020, 5 May 2020, 16 May 2020, 28 May 2020, 7 June 2020, 19 June 2020, 7 July 2020, and 17 July 2020). Under I1 treatment for example (Figure 5a), the peak duration corresponding to each irrigation was synchronous with the irrigation period, and the peak value was significantly correlated with the irrigation amount. That is, the greater the irrigation amount, the higher the SWC peak value. The SWC peak values corresponding to the irrigation amounts of 90, 180, 270, and 210 mm were 25.67, 28.12, 30.28, and 27.70%, respectively, within two to three days after irrigation.

Following each irrigation, the SWC decreased significantly due to evapotranspiration, fruit tree uptake, and transport to subsoils [20,30,31], after which the decreasing trend in water content slowed. The average soil water content exhibited a consistent pattern of change across all layers and treatments throughout each growth stage. Specifically, from the bud swelling stage to the flowering stage, the almond tree leaves were not fully expanded, resulting in water consumption being primarily driven by inter-tree evaporation. Additionally, the low air temperature and weak solar radiation further contributed to reduced water consumption during this period. Irrigation was applied regularly during the young fruit stage, characterized by a fully developed tree canopy, elevated ground cover, low inter-tree evaporation, and high plant transpiration [33], which is a crucial period for water demand in the growth of Badam fruits. Subsequently, as the fruits reached maturity, irrigation was reduced, and soil water content tended to decline.

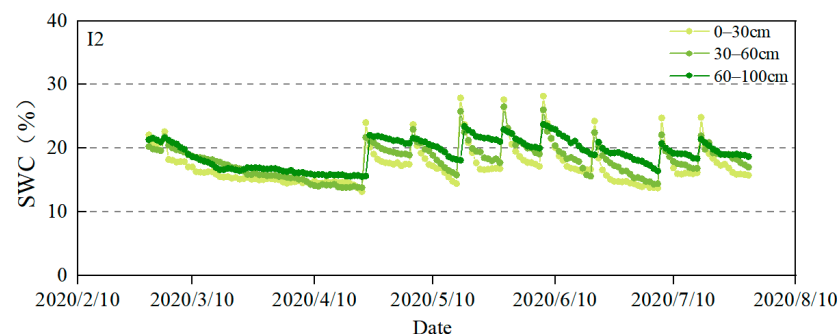
It was also observed that SWC correlated with the depth of the soil layer. That is, the SWC increased with the depth of the soil layer, and its variation synchronized with a certain relative difference. Almond trees are shallow-rooted plants with vertical root distribution within 1 m, and the main root system is distributed at depths of 20–70 cm from the surface [34]. Therefore, this study focused on analyzing changes in soil moisture within the 0–100 cm range. A moist layer slightly below the main root distribution area can encourage deeper root growth, increasing wind resistance and nutrient availability to the plant, thereby increasing the ability of the root to absorb and utilize nutrients. For this experiment, the increase in root soil moisture after each irrigation event was roughly



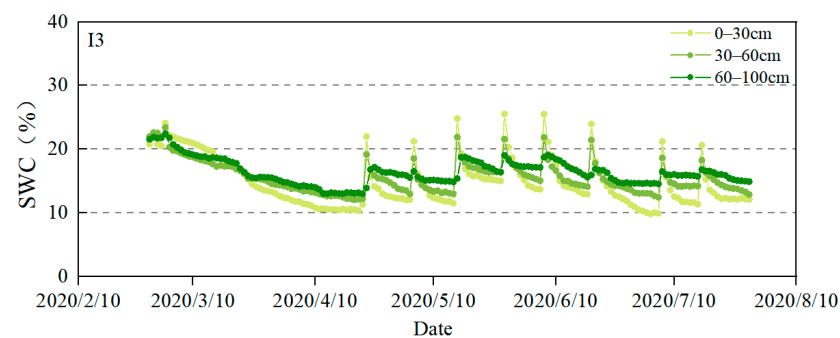
consistent with the amount of irrigation water, and the SWC of the deep soil after irrigation did not exceed the field water holding capacity, so there was no obvious deep leakage during irrigation. In the experiment, soil moisture sensor measurements at a depth of 80 cm below the surface were used to calculate soil moisture content at a depth of 0–100 cm. The root system of the nine-year-old almond tree can reach about 90 cm underground, so the soil moisture detected by the soil moisture sensor at the lowest point gradually decreased over time due to the water absorption of the root system. In addition, since the root system of almond trees is mainly distributed at a depth of 20–70 cm, the moisture content of the soil layer at a depth of 30–60 cm decreased due to the water absorption of the root system, and the soil matric potential increased. At the same time, the water in the soil layer at a depth of 60–100 cm was replenished, driven by capillary action and water potential, which may also lead to a decrease in soil moisture content at the lowest point [35].



(a) I1 irrigation treatment



(b) I2 irrigation treatment



(c) I3 irrigation treatment

**Figure 5.** Variations of the soil water content (SWC) in soil layers at different depths under I1, I2, and I3 irrigation treatments.

### 3.1.2. Leaf Area Index and Chlorophyll Content

The variations in LAI and SPAD values of almond trees during the growth stages are shown in Figure 6. It can be seen that both parameters exhibit an overall gradually increasing trend. As shown in Figure 6a, the LAI value was zero when the leaves in the canopy were in the sprouting state at the bud swelling stage of almond trees. As the

weather warmed up, the canopy grew and developed, and the leaves grew rapidly with LAI increasing from 0.7–1.1 at flowering stage to 2.8–4.0 at young fruit stage. After the young fruit stage, the nutritive growth phase of almond tree ended, and the reproductive growth phase began. The plant began to transport nutrients primarily to the fruit, leading to a gradual slowdown in canopy leaf growth. Therefore, LAI remained at a relatively stable level (3.3–4.5) throughout fruit expansion and maturation. Under different irrigation treatments, the canopy LAI of almond trees gradually differed with plant growth. The LAI from the young fruit stage to the maturation stage was ranked in the order of I1 (4.0–4.5) > I2 (3.6–3.9) > I3 (2.8–3.5). This suggests that SWC had a significant effect on canopy leaf growth. Although the overall trend for SPAD (Figure 6b) was similar to that of LAI, there was no significant difference in the SPAD values under different SWC values, suggesting that the canopy chlorophyll content measured using the SPAD instrument did not effectively reflect the changes in the moisture content in the almond trees' environment.

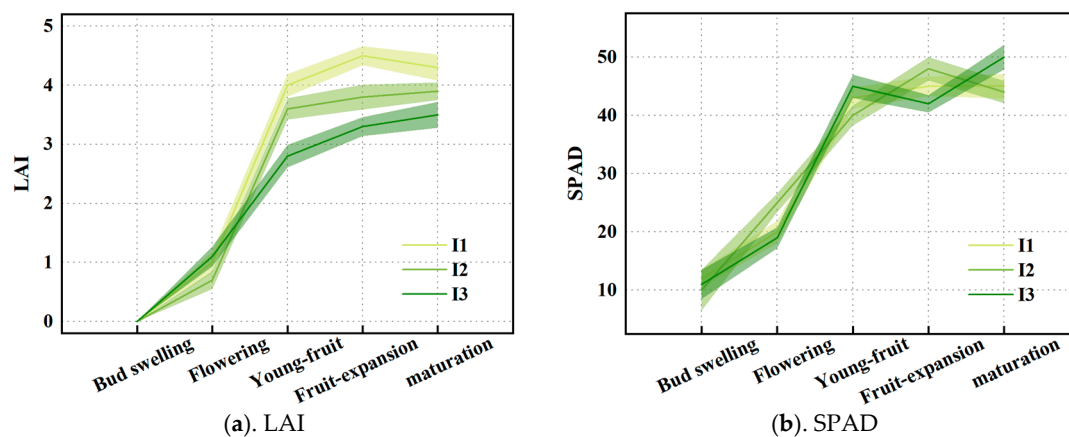


**Figure 6.** Variations in LAI and SPAD values of the almond tree canopy at each growth stage under irrigation treatments I1, I2, and I3.

### 3.1.3. Canopy/Air Temperature Difference

The variations in canopy/air temperature difference ( $\Delta T$ ) throughout the growth period of the sampled almond trees in this experiment are shown in Figure 7. The experimental observations were initiated at the bud swelling stage when the leaves were young ( $LAI \approx 0$ ) and their physiological activities were relatively slow, which did not permit effective transpiration. Under sunlight (10:00–14:00), the solar radiation absorbed by the canopy of almond trees was converted into heat energy [18]. Therefore, the canopy temperature at the bud swelling stage was higher than the air temperature [19], i.e., the  $\Delta T$  at this stage was approximately  $1\text{ }^{\circ}\text{C}$ . As the leaves of almond trees fully developed ( $LAI \geq 2.5$ ), the canopy transpiration rate normalized, which converted liquid water into gaseous water vapor while consuming heat, resulting in a reduction of leaf temperatures. Therefore, the  $\Delta T$  of almond trees decreased gradually ( $\Delta T < -2\text{ }^{\circ}\text{C}$ ) from the flowering stage to the maturation stage. From the bud swelling stage to young fruit stage, canopy leaves grew rapidly, and LAI increased to 2.8–4.0, causing  $\Delta T$  to rapidly decrease from 0.7–1.2  $^{\circ}\text{C}$  to values between  $-5.6$  and  $-3.95\text{ }^{\circ}\text{C}$ . During subsequent growth, almond trees shifted from the nutrient growth phase to the reproductive growth phase, in which the leaf development rate slowed, and the overall canopy leaves were maintained in a stable state. Consequently, the  $\Delta T$  value of almond trees was maintained between  $-5.6$  and  $-3.1\text{ }^{\circ}\text{C}$  from the young fruit stage to maturation stage.

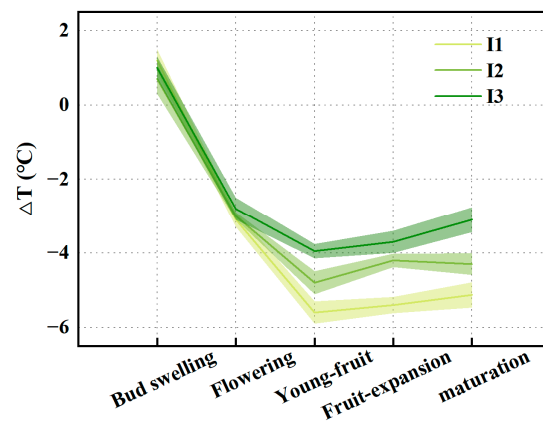


**Figure 7.** Variations in the canopy/air temperature difference ( $\Delta T$ ) of almond trees at each growth stage under irrigation treatments I1, I2, and I3.

As shown in Figure 7, different irrigation treatments had significant effects on the  $\Delta T$  of almond trees, where differences in  $\Delta T$  between different soil water environments were lower at early growth stages (i.e., bud swelling and flowering stages) when the canopy leaves were young ( $LAI \leq 1.1$ ). As trees grew, almond trees with adequate water supply had greater leaf area values;  $LAI$  was the highest under I1 treatment, followed by I2, and then I3 ( $I1 > I2 > I3$ ). Additionally, transpiration was more intense in trees irrigated with higher amounts of water [8]. As a result, the  $\Delta T$  between different irrigation treatments gradually widened from the young fruit stage to the maturation stage. Overall,  $\Delta T$  was the lowest in I1 treatment, followed by I2 and I3. That is,  $I1 (-5.6 \text{ to } -5.1 \text{ } ^\circ\text{C}) < I2 (-4.8 \text{ to } -4.3 \text{ } ^\circ\text{C}) < I3 (-3.95 \text{ to } -3.1 \text{ } ^\circ\text{C})$ .

To understand the changing pattern of the  $\Delta T$  of almond trees in-depth, canopy temperature was monitored throughout the day on a typical sunny day (1 July 2020, Figure 8a) and a typical cloudy day (28 June 2020, Figure 8b). The sample plants under I1 treatment on these two days were at the maturation stage and were characterized by more stable physiological activities [36,37]. Therefore, the daily variation in their canopy temperature is relatively representative. The changing trends of the  $\Delta T$  and PAR of almond trees in the sunny environment presented in Figure 8a show an overall increasing trend first, then decreasing, and increasing again. Combined with the trend plot of photosynthetically active radiation values, data show that solar radiation was 0 during nighttime (0:00–6:00), the canopy temperature did not differ much from the air temperature, and  $\Delta T$  was approximately  $0 \text{ } ^\circ\text{C}$ . As the sun rose, the light radiation received by the canopy was converted into heat, leading to a gradual increase in  $\Delta T$ . At approximately 8:00, the canopy began transpiration, and water volatilized by absorbing part of the heat, resulting in a gradual decrease in canopy temperature. As solar radiation was too strong after 12:00, the leaf stomata of the canopy were partially closed [38], and transpiration was relatively reduced, causing an increase in  $\Delta T$ . After 16:00, the intensity of solar radiation weakened, the leaf stomata reopened, and the effect of canopy transpiration increased, causing a slight decrease in  $\Delta T$ . After 18:00, with sunset, the intensity of sunlight and transpiration decreased, resulting in a gradual increase in  $\Delta T$  until it eventually returned to near  $0 \text{ } ^\circ\text{C}$ . The variation trend of  $\Delta T$  on the cloudy day was approximately the same as that on the sunny day. However, the variations in  $\Delta T$  values were lesser on the cloudy day ( $5.4 \text{ } ^\circ\text{C}$ ) than those on the sunny day ( $12.3 \text{ } ^\circ\text{C}$ ), which was due to the weaker intensity of solar radiation and the reduced transpiration on the cloudy day. The heat absorbed by the canopy on the cloudy day was reduced, ultimately resulting in a higher  $\Delta T$  ( $-3.9 \text{ to } 1.5 \text{ } ^\circ\text{C}$ ) than that on the sunny day ( $-8.8 \text{ to } 3.5 \text{ } ^\circ\text{C}$ ). Regardless of whether the days were sunny or cloudy, the all-day  $\Delta T$  under different irrigation treatments also showed a trend similar to that of  $\Delta T$  on sunny days (Figure 8a); that is,  $I1 < I2 < I3$ . It can be seen that the effect of soil water content on the  $\Delta T$  of almond trees was consistent throughout plant

growth, but the significance of its effect on the  $\Delta T$  still needs to be further analyzed in the following sections.

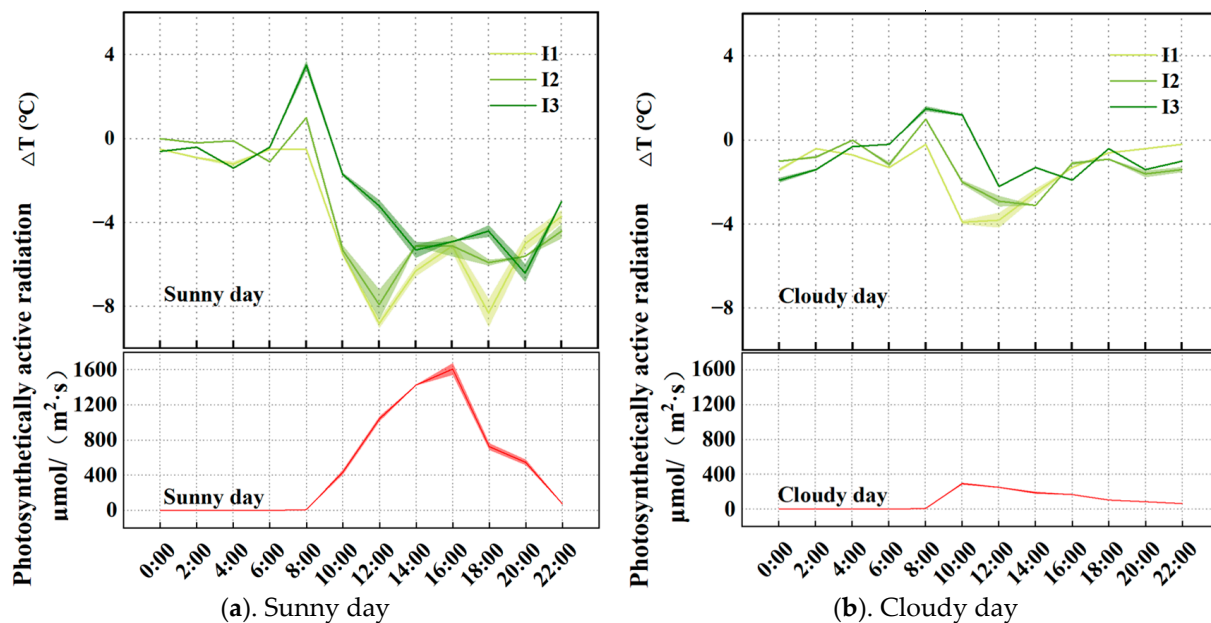


**Figure 8.** Variations in the canopy/air temperature difference ( $\Delta T$ ) of almond trees at the maturation stage under I1, I2, and I3 irrigation treatments on sunny and cloudy days.

#### 3.1.4. Trunk Diameter Variation

Thermal effect and transpiration are among the factors causing the variations in plant trunk diameter. Under optimal weather conditions, the solar radiation absorbed by plants is converted into heat energy, which causes a minor swelling of water-storing organs. This is an external manifestation of the thermal effect in plants [28]. In addition, the transpiration rate of plants at midday is generally greater than the water uptake rate by the root system [20]. To meet the demand of the canopy transpiration, the water stored in each organ (root, stem, and fruit) of a plant begins to flow towards its leaves, which leads to a shrinkage of these organs. Thus, the external manifestation of shrinkage in the plant trunk is the result of a dynamic balance between thermal effect and transpiration.

The variations in the trunk shrinkage of almond trees throughout the growth period are presented in Figure 9. The trunk diameter exhibited an overall shrinking trend due to the significant transpiration effect during the sampling period of 10:00–14:00. The TDS increased to varying degrees as plants grew under each irrigation treatment. This is because in winter and early spring, plant transpiration and tissue growth were weaker, and the midday thermal effect expanded the volume of plant organs, partially counteracting the trunk shrinkage. In summer, the trunk growth of adult almond trees slowed, and the variation in their volumes was primarily caused by water exchange between plant tissues. The TDS values at each growth stage were as follows: bud swelling stage (178.667–220.852  $\mu\text{m}$ ) < flowering stage (190.742–298.571  $\mu\text{m}$ ) < young fruit stage (208.574–353.390  $\mu\text{m}$ ) < fruit expansion stage (212.342–366.317  $\mu\text{m}$ ) < maturation stage (226.387–405.539  $\mu\text{m}$ ). In addition, the TDS values under different irrigation treatments were as follows: I1 (201.896–226.387  $\mu\text{m}$ ) < I2 (178.667–298.571  $\mu\text{m}$ ) < I3 (220.852–405.501  $\mu\text{m}$ ). This trend occurred because the amount of water that a plant can absorb from the soil directly affects its internal water content and indirectly affects the volume variation of plant organs [21,27,39]. Reduced water availability in the soil under the irrigation treatments with lower amounts of water (I2 and I3) reduced the rate of water uptake by the root system of plants. This increased the temporary deficit of water in the plant body, which in turn exacerbated the shrinkage of the water-storing organs in almond trees. Ultimately, the

higher the utilization of the water stored in the trunk under I2 and I3 treatments, the greater the daily shrinkage.

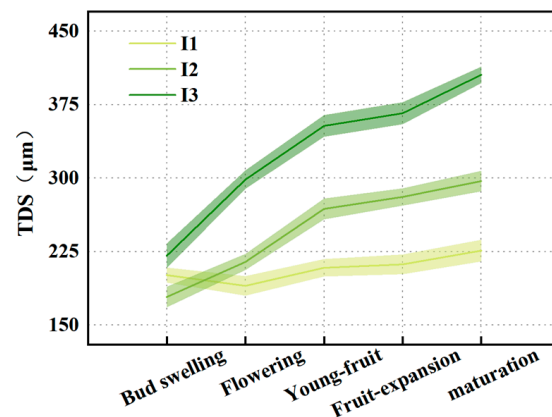


**Figure 9.** Variations in the trunk diameter shrinkage (TDS) of almond trees at each growth stage under irrigation treatments I1, I2, and I3.

The daily variation in the trunk diameter of almond trees on both sunny (Figure 10a) and cloudy (Figure 10b) days exhibited a good periodicity, and the daily variation curve showed an overall increasing, then decreasing, and again increasing trend. This periodic shrinking/swelling variation in trunk diameter was mainly due to transpiration. The transpiration rate of almond trees changed according to increases or decreases in solar radiation, which in turn caused shrinkage and swelling of the trunk diameter. In particular, at nighttime (22:00 on day 1 to 8:00 the next day), the transpiration intensity was weak, the water absorption rate of the root system was greater than the transpiration rate, and the water deficit in water-storing organs during the daytime was replenished. Therefore, the volumes of the root, stems, and fruit were recovered and began to swell, implying that the trunk diameter variation showed an opposite trend to that of solar radiation. Compared with the daily trunk diameter variation ( $-278$  to  $122$   $\mu\text{m}$ ) in the sunny environment (maximum PAR =  $1610$   $\mu\text{mol m}^{-2} \text{s}^{-1}$ ), the daily trunk diameter variation ( $-182$  to  $94$   $\mu\text{m}$ ) in the cloudy environment (maximum PAR =  $294$   $\mu\text{mol m}^{-2} \text{s}^{-1}$ ) was more moderate, which further demonstrated the effect of solar radiation on the shrinkage and swelling of the plant trunks. In addition, the daily trunk diameter variations under different irrigation treatments were ranked in a sequence of  $I1 < I2 < I3$  under both sunny and cloudy environments, but the trunk shrinkage was less under cloudy conditions, which was attributed to the lower intensity of transpiration and the lower water consumption rate of almond trees on cloudy days.

### 3.1.5. Fruit Diameter Variation

The variations in the FDS of almond trees are shown in Figure 11, which are similar to those in the TDS both during the whole growth period and on a single-day scale. That is, the FDS gradually increased from the young fruit stage to the maturation stage and was ranked in the order of  $I1 < I2 < I3$  under different irrigation treatments. On a single-day scale, almond fruit also exhibited an initial swelling process, followed by shrinking and swelling; the FDS under different irrigation treatments was also ranked in a sequence of  $I1 < I2 < I3$ .

In addition, the maximum fruit shrinkage under sunny conditions was also greater than that under cloudy conditions, as shown in Figure 12. The variation in fruit diameter was similar to that in trunk diameter because almond fruit, a water-storing organ, participates in the water transport process related to transpiration together with the trunk. That is, the variation in the volume of the plant's water-storage organs during the day was actually a balance between two basic biological processes: the exchange of water between its tissues and its physiological growth and the thermal effect [29]. However, the difference in the

variation in fruit diameter ( $-590$  to  $100 \mu\text{m}$ ) was much greater than that in trunk diameter ( $-278$  to  $122 \mu\text{m}$ ), which was due to the greater variation in water content within the fruit compared to the trunk. As the water content of the trunk decreased, the mature xylem therein hardly deformed, whereas the immature xylem, phloem, and other associated water-storing tissues shrank. Moreover, when the water content of the fruit decreased, the fruit shrank more than the trunk due to the lack of support, similar to the xylem in the trunk [40].

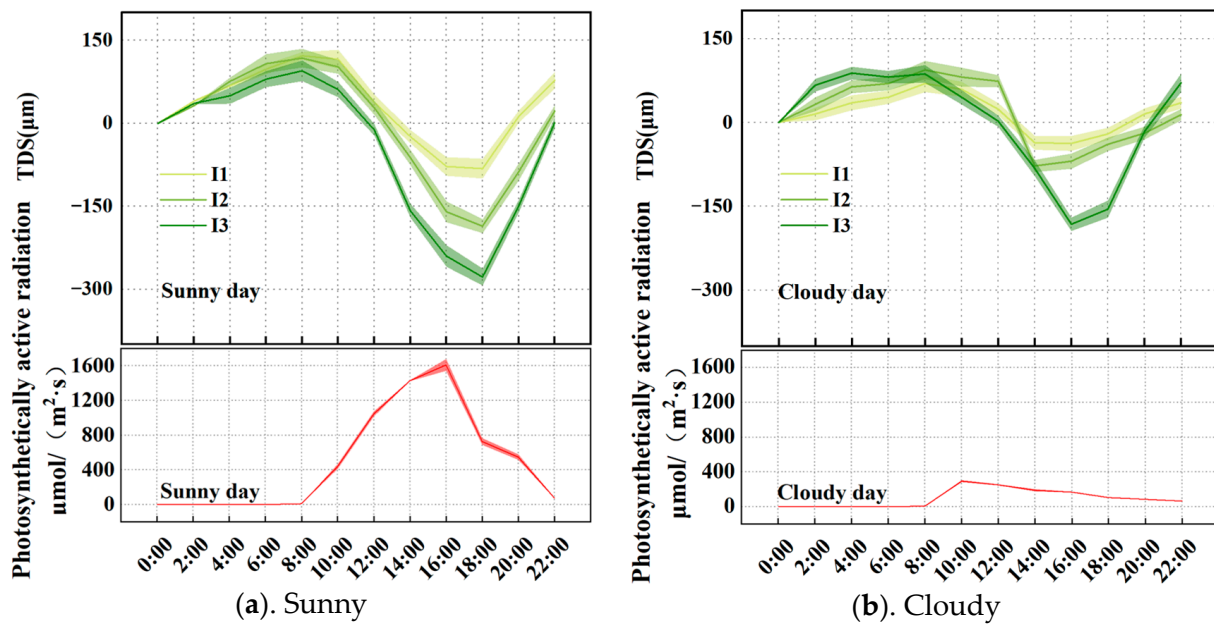


**Figure 10.** Variations in the trunk diameter shrinkage (TDS) of almond trees at the maturation stage under irrigation treatments I1, I2, and I3 on sunny and cloudy days.

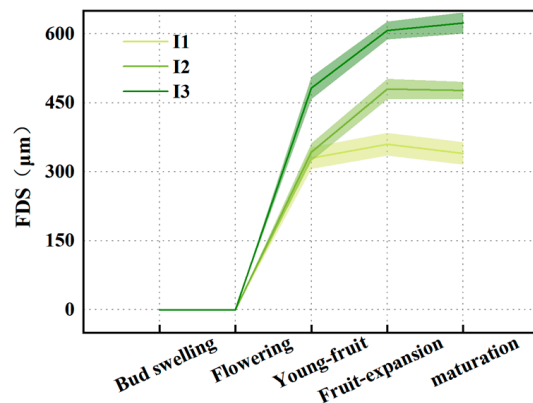


**Figure 11.** Variations in the fruit diameter shrinkage (FDS) of almond trees at each growth stage under irrigation treatments I1, I2, and I3.

In addition, variations in the fruit volume were closely related to the growth stages [41]. Young fruit shrank significantly during the daytime because their water was highly mobile due to the low content of soluble solids in the fruit. In contrast, the water content of mature fruit was lower, which limited the outflow of water from the fruit. As a result, the volumetric shrinkage of fruit during the maturation stage was slightly reduced under water stress conditions.

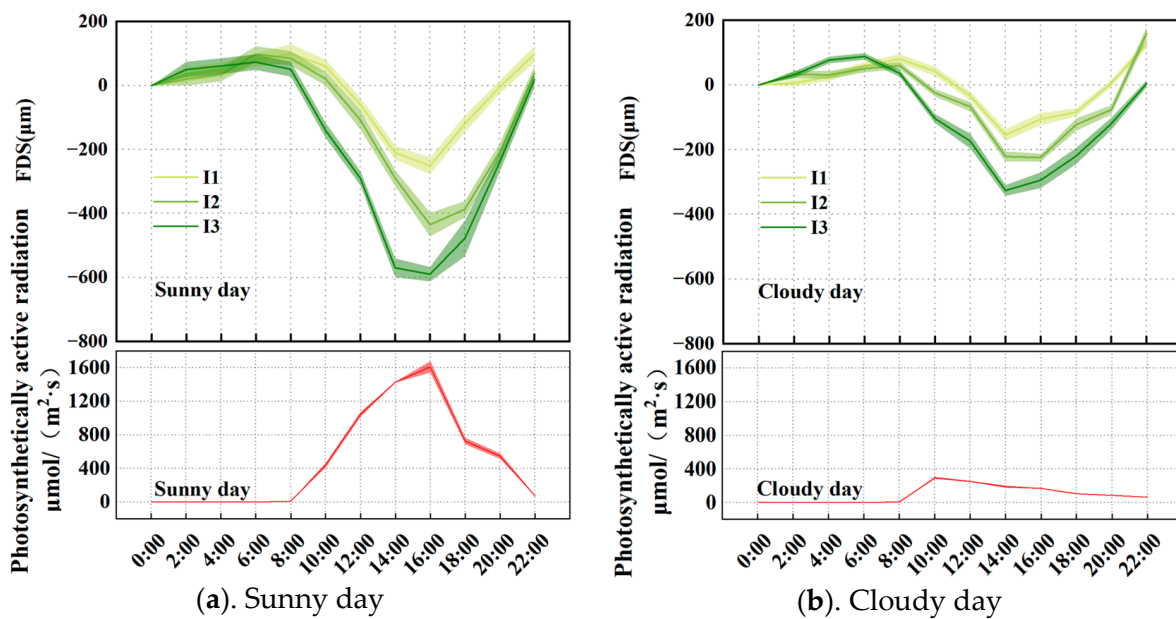


**Figure 12.** Variations in the fruit diameter shrinkage (FDS) of almond trees at the maturation stage on sunny and cloudy days under irrigation treatments I1, I2, and I3.

### 3.2. Variations in Responses of Almond Trees to Irrigation

To better analyze the response of almond trees to different irrigation treatments, the changes in major physiological parameters were summarized in relation to irrigation treatments. As shown in Figure 13, all physiological parameters except SPAD were significantly correlated with irrigation treatments. Among them, fruit yield and canopy LAI decreased as the amount of water for irrigation reduced;  $\Delta T$ , TDS, and FDS increased with the increasing irrigation amount. The correlations (correlation coefficient  $r$ ) between the main physiological parameters and the irrigation amount at each growth stage are also shown in Figure 13. During the early growth stages (bud swelling and flowering), only the TDS was negatively correlated with the irrigation amount ( $r = -0.470$  to  $-0.953$ ). This was because the water treatment experiment had just started, and the physiological activity of almond trees was weak in the spring. With the onset of summer, solar radiation gradually increased, leaves and fruits continued to grow, and all physiological activities of the plants became more active. In addition, correlations among the parameters peaked at the maturation stage. Specifically,  $\Delta T$ , TDS, and FDS showed significantly negative correlations with irrigation treatment and fruit yield ( $r = -0.949$  to  $-0.996$ ). Significant positive correlations ( $r = 0.953$ – $0.978$ ) were observed between  $\Delta T$ , TDS, and FDS. The correlation coefficients indicate that when the irrigation amount was reduced, canopy LAI, fruit yield, and trunk/fruit volume decreased, and canopy temperature increased accordingly. However, the SPAD value did not change significantly.

Because the daily variations in  $\Delta T$ , TDS, and FDS were obvious, it was necessary to determine their sensitivity to the irrigation amount during different time periods. It can be seen from Table 3 that under sunny conditions,  $\Delta T$  was significantly correlated with the irrigation amount from 8:00–18:00 ( $r = -0.991$  to  $-0.778$ ), and so were the TDS from 4:00 to 22:00 ( $r = 0.676$ – $0.998$ ) and FDS from 8:00 to 22:00 ( $r = 0.758$ – $0.999$ ). Under cloudy conditions,  $\Delta T$ , TDS, and FDS were also significantly correlated with the irrigation amount from 8:00 to 14:00 ( $r = -0.997$  to  $-0.655$ ), from 14:00 to 20:00 ( $r = 0.827$ – $0.904$ ), and from 8:00 to 20:00 ( $r = 0.783$ – $0.992$ ), respectively. Overall, the moisture-sensitive periods of the three measured parameters were correlated with the intensity of solar radiation and transpiration.



**Figure 13.** Correlations (correlation coefficient  $r$ ) between parameters such as fruit yield, canopy LAI, relative chlorophyll content (SPAD), canopy/air temperature difference ( $\Delta T$ ), trunk diameter shrinkage (TDS), and fruit diameter shrinkage (FDS) of almond trees at critical growth stages. Note: \* indicates the values are significant at the probability level  $p < 0.05$ ; \*\* indicates that the values are distinctly significant at the probability level  $p < 0.01$ .



**Table 3.** Correlation coefficients of irrigation volume of canopy/air temperature difference ( $\Delta T$ ), trunk diameter shrinkage (TDS), and fruit diameter shrinkage (FDS) with the irrigation amount for almond trees during the whole day under different weather conditions.

Time period		0:00	2:00	4:00	6:00	8:00	10:00
Sunny day	$\Delta T$	0.156 NS	−0.286 NS	−0.380 NS	−0.132 NS	−0.990 **	−0.888 **
	TDS	0.000 NS	0.500 NS	0.676 *	0.634 *	0.747 *	0.762 *
	FDS	0.000 NS	−0.500 NS	−0.421 NS	0.271 NS	0.758 *	0.943 **
Time period		12:00	14:00	16:00	18:00	20:00	22:00
Sunny day	$\Delta T$	−0.913 **	−0.778 **	−0.866 **	−0.991 **	0.401 NS	−0.500 NS
	TDS	0.825 *	0.970 **	0.997 **	0.998 **	0.991 **	0.725 *
	FDS	0.948 **	0.952 **	0.999 **	0.962 **	0.851 *	0.644 *
Time period		0:00	2:00	4:00	6:00	8:00	10:00
Cloudy day	$\Delta T$	0.554 NS	0.493 NS	−0.569 NS	−0.220 NS	−0.973 **	−0.989 **
	TDS	0.000 NS	−0.267 NS	−0.466 NS	−0.525 NS	−0.507 NS	0.394 NS
	FDS	0.000 NS	−0.365 NS	−0.303 NS	−0.233 NS	0.828 *	0.940 **
Time period		12:00	14:00	16:00	18:00	20:00	22:00
Cloudy day	$\Delta T$	−0.997 **	0.655 *	−0.577 NS	−0.397 NS	0.138 NS	0.367 NS
	TDS	0.292 NS	0.904 **	0.951 **	0.923 **	0.827 **	−0.413 NS
	FDS	0.957 **	0.992 **	0.989 **	0.970 **	0.783 *	0.570 NS

Note: In this table, \* indicates that the values are significant at the probability level  $p < 0.05$ ; \*\* indicates the values are distinctly significant at the probability level  $p < 0.01$ .

#### 4. Discussion

In this study, a field (in-situ) monitoring system for almond trees was constructed using various sensors. This system continuously monitored the physiological responses of the almond trees in a non-destructive manner and exhibited good reliability. According to the monitoring results of the sensor system, canopy LAI [40],  $\Delta T$  [8], trunk shrinkage [29], and fruit shrinkage [42] were more sensitive to water deficit. The findings of this study support the assertion made by Li et al. [28] that poplar trunks undergo contraction during daylight hours and expansion during nighttime; specifically, the gradual contraction between 8:00 and 16:00. The results of this study confirm a similar pattern of contraction and expansion in almond (Badam) tree trunks occurring at approximately the same times of the day. This study revealed that the variation in canopy temperature is strongly correlated with the level of water stress, particularly around midday (12:00). This finding aligns with the research conducted by Candon et al. [8] during the time frame from 11:00 to 14:20. Additionally, it was observed that fruit trees experiencing adequate water supply exhibited lower canopy/air temperature differences, which can be attributed to the delayed closure of stomata in well-watered leaves. Rosa et al. [21], in their study on nectarine, found that the TDS value increased with the increase of water requirement, and the TDS of the water deficit treatment and the sufficient water treatment were about 300  $\mu\text{m}$  and 200  $\mu\text{m}$ , respectively,

during the whole life span. The TDS of almond (Badam) trees exhibited a pattern similar to the above studies of changes throughout their entire lifespan in the present study. This pattern can be attributed to the gradual growth of trunks. Specifically, the TDS reached its minimum value in March and its maximum value in July. The TDS values ranged from 221–406  $\mu\text{m}$  for the deficit treatment to 179–226  $\mu\text{m}$  for the well-watered treatment. In a similar study, Giron et al. [29] examined the impact of varying water stress conditions on the canopy/air temperature difference, trunk diameter, and fruit diameter of citrus trees. Their findings revealed that reducing irrigation water by 50% resulted in a notable increase of approximately 5 °C in the canopy temperature of citrus trees. Additionally, the gradual intensification of transpiration between 9:00 and 17:00 h led to a contracted state in both trunk and fruit diameter. These conclusions align closely with the observations of the present study. Based on the trunk diameter changes, Palomo et al. [20], Malheiro et al. [27], and Giron et al. [39] investigated the changing trend of indicators such as the trunk growth rate, daily maximum shrinkage, daily net growth, daily variation of trunk diameter, and time required for complete recovery on the same day under water deficit. All the above indicators are important for measuring the water deficit in plants. Therefore, further research is needed in subsequent experiments on almond trees to calculate the trunk and fruit diameter variations and corresponding parameters over different time periods under real-time observation.

In this study, the sensitivity of  $\Delta T$ , TDS, and FDS to soil water deficit under different weather conditions was determined. Considering the short duration of solar radiation under cloudy conditions and the insufficient changes in the values of the main physiological parameters of almond trees, the time period from 14:00 to 18:00 under sunny conditions was considered suitable for measuring the  $\Delta T$ , TDS, and FDS of almond trees during actual production growth stages. Data analysis of the results in Section 3 indicated that all the above parameters were also closely related to fruit yield at the maturation stage [36,42]. As Corell et al. [41] found that, olive fruits are sensitive to water stress, and a water deficit leads to a reduction in fruit size, which further affects yield. Thus, parameters such as canopy LAI,  $\Delta T$ , trunk shrinkage, and fruit shrinkage can also be used to estimate the degree of water deficit in almond trees in real time. In their study, Ballester et al. [18] asserted that canopy temperature is strongly correlated with physiological processes, including the stomatal regulation of transpiration and the evaporative cooling of leaves. This relationship enables a more direct evaluation of plant water status, thereby proposing its utilization in conjunction with trunk diameter variations as an indicator of water stress. It follows that multi-source monitoring systems integrating the information of crop evapotranspiration [31], stem water potential [28], and canopy phenology imaging [18] will certainly play a greater role in the future [43].

Although in-situ tests were conducted in the field during the growth period of almond trees for a single year (2020), which was characterized as a median water year using meteorological data, the experimental data and conclusions presented herein serve as a valuable reference for assessing the water deficit of almond trees in the Xinjiang region. Nevertheless, there is a need to repeat irrigation experiments in subsequent years to further optimize the sensor combinations [44], establish a reliable and accurate monitoring system [44], and carry out studies on water deficit diagnosis [45]. For example, it is necessary to understand how to enable sensors to simultaneously monitor the canopies of multiple almond trees in a reasonable and convenient way for longer durations, and how to choose representative trunks or fruits, to better capture the diameter shrinkage/swelling variations. It is also recommended to calculate crop coefficients of almond (Badam) orchards [46], estimate daily evapotranspiration [47], or construct a moisture decision model for almond trees using machine learning algorithms [48].

## 5. Conclusions

In this study of the median water year, we developed a non-destructive physiological information monitoring system consisting of the soil moisture sensor, infrared thermometer,

plant canopy analyzer, chlorophyll meter, trunk diameter sensor, and fruit diameter sensor to measure the soil water content in the root region,  $\Delta T$ , LAI, SPAD, trunk diameter, and fruit diameter of almond trees. During the experiment, measurements of multiple growth parameters in different water supply environments confirmed good reliability of the system. The results of the median water year showed that under the irrigation levels corresponding to 100%, 75%, and 50% of  $ET_c$ ,  $\Delta T$ , TDS, and FDS exhibited significant negative correlations ( $r = -0.949$  to  $-0.996$ ) with the irrigation treatment and yield parameters. Additionally, significant positive correlations ( $r = 0.953$ – $0.978$ ) were found between  $\Delta T$ , TDS, and FDS. The above correlation coefficients indicate that when the irrigation amount was reduced, canopy LAI, fruit yield, and diameter of trunk and fruit decreased, and the canopy temperature increased accordingly. However, the SPAD content did not show significant change. In addition, the variations in the main parameters during the course of a single day suggest that the time period from 14:00 to 18:00 under sunny conditions is appropriate for measuring the  $\Delta T$ , TDS, and FDS in the canopies of almond trees for effective real-time production monitoring. This is because the results of the measurements during this period were significantly correlated with the amount of water used for irrigation ( $|r| \geq 0.778$ ). The findings of this study can provide technical suggestions and guidance for constructing and establishing a water deficit diagnosis and monitoring system for almond trees in Xinjiang, China.

**Author Contributions:** H.Y.: Data analysis, Chart drawing, Article writing. Y.S.: Data processing. Y.C.: Data collection. Y.M.: Data collection. X.W.: Data collection. M.R.S.: Article revision. Y.Z.: Experimental design, Article revision. X.H.: Experimental design, Article revision. All authors have read and agreed to the published version of the manuscript.

**Funding:** This research was funded by Academy of Agricultural Sciences Youth Science and Technology Backbone Innovation Ability Training Project (XJNKQ-2020018).

**Data Availability Statement:** Data will be available on request.

**Conflicts of Interest:** The authors declare no conflict of interest.

## References

- Gupta, A.; Sharma, R.; Almond, S.S. *Antioxidants in Vegetables and Nuts—Properties and Health Benefits*; Springer: Singapore, 2020; pp. 423–452.
- Salgado-Ramos, M.; Martí-Quijal, F.J.; Huertas-Alonso, A.J.; Sánchez-Verdú, M.P.; Barba, F.J.; Moreno, A. Almond hull biomass: Preliminary characterization and development of two alternative valorization routes by applying innovative and sustainable technologies. *Ind. Crops Prod.* **2022**, *179*, 114697. [[CrossRef](#)]
- Moldero, D.; López-Bernal, Á.; Testi, L.; Lorite, I.J.; Fereres, E.; Orgaz, F. Long-term almond yield response to deficit irrigation. *Irrig. Sci.* **2023**, *1*, 409–420. [[CrossRef](#)]
- Espadafor, M.; González-Dugo, V.; Orgaz, F.; Testi, L.; López, M.; Fereres, E. Water relations in almond trees under moderate water deficits. *Acta Hort.* **2017**, *1150*, 113–118. [[CrossRef](#)]
- Martín-Palomo, M.J.; Andreu, L.; Pérez-López, D.; Centeno, A.; Galindo, A.; Moriana, A.; Corell, M. Trunk growth rate frequencies as water stress indicator in almond trees. *Agric. Water Manag.* **2022**, *271*, 107765. [[CrossRef](#)]
- Huang, Y.; Ren, Z.; Li, D. Phenotypic techniques and applications in fruit trees: A review. *Plant Methods.* **2020**, *16*, 107. [[CrossRef](#)]
- Wang, G.; Ma, H.; Gulina, T. Correlation Between Soil and Plant Geochemical Characteristics and Environmental Quality Research in Shache Almonds Planting Area. *Geol. Xinjiang* **2020**, *38*, 412–416.
- David, G.; Mathieu, V.; Sébastien, M.; Labbé, S.; Delalande, M.; Regnard, J.L. Unravelling the responses of different apple varieties to water constraints by continuous field thermal monitoring. *Sci. Hortic.* **2022**, *299*, 111013.
- Jones, H.G. Irrigation scheduling: Advantages and pitfalls of plant-based methods. *J. Exp. Bot.* **2023**, *55*, 2427. [[CrossRef](#)]
- Cuevas, M.V.; Martín-Palomo, M.J.; Diaz-Espejo, A.; Torres-Ruiz, J.M.; Rodríguez-Dominguez, C.M.; Perez-Martin, A.; Pino-Mejías, R.; Fernández, J.E. Assessing water stress in a hedgerow olive orchard from sap flow and trunk diameter measurements. *Irrig. Sci.* **2013**, *31*, 729–746. [[CrossRef](#)]
- Morandi, B.; Manfrini, L.; Zibordi, M.; Losciale, P.; Grappadelli, L.C. Effects of drought stress on the growth, water relations and vascular flows of young ‘summerkiwi’ fruit. *Acta Hort.* **2011**, *9*, 355–359. [[CrossRef](#)]
- José, F. Plant-Based Methods for Irrigation Scheduling of Woody Crops. *Horticulturae* **2017**, *3*, 35.
- Meng, Z.; Duan, A.; Chen, D.; Dassanayake, K.B.; Wang, X.; Liu, Z.; Liu, H.; Gao, S. Suitable indicators using stem diameter variation-derived indices to monitor the water status of greenhouse tomato plants. *PLoS ONE* **2017**, *12*, 1423. [[CrossRef](#)] [[PubMed](#)]

14. Montoro, A.; Fereres, E.; López-Urrea, R.; Mañas, F.; López-Fuster, P. Sensitivity of Trunk Diameter Fluctuations in *Vitis vinifera* L. Tempranillo and Cabernet Sauvignon Cultivars. *Am. J. Enol. Vitic.* **2012**, *63*, 85–93. [[CrossRef](#)]
15. Cifre, J.; Bota, J.; Escalona, J.M.; Medrano, H.; Flexas, J. Physiological tools for irrigation scheduling in grapevine (*Vitis vinifera* L.): An open gate to improve water-use efficiency? *Agric. Ecosyst. Environ.* **2005**, *106*, 159–170. [[CrossRef](#)]
16. Escalona, J.; Flexas, J.; Medrano, H. Drought effects on water flow, photosynthesis and growth of potted grapevines. *Vitis J. Grapevine Res.* **2002**, *41*, 57–62.
17. Ali, A.; David, C. Use of crop water stress index for monitoring water status and scheduling irrigation in wheat. *Agric. Water Manag.* **2001**, *47*, 69–75.
18. Ballester, C.; Castel, J.; Jiménez-Bello, M.A.; Castel, J.R.; Intrigliolo, D.S. Thermographic measurement of canopy temperature is a useful tool for predicting water deficit effects on fruit weight in citrus trees. *Agric. Water Manag.* **2013**, *122*, 1–6. [[CrossRef](#)]
19. Vantyghem, M.; Merckx, R.; Stevens, B.; Hood-Nowotny, R.; Swennen, R.; Dercon, G. The potential of stable carbon isotope ratios and leaf temperature as proxies for drought stress in banana under field conditions. *Agric. Water Manag.* **2022**, *260*, 107247. [[CrossRef](#)]
20. Martín-Palomo, M.; Corell, M.; Andreu, L.; López-Moreno, Y.; Galindo, A.; Moriana, A. Identification of water stress conditions in olive trees through frequencies of trunk growth rate. *Agric. Water Manag.* **2021**, *247*, 106735. [[CrossRef](#)]
21. De la Rosa, J.; Domingo, R.; Gómez-Montiel, J.; Pérez-Pastor, A. Implementing deficit irrigation scheduling through plant water stress indicators in early nectarine trees. *Agric. Water Manag.* **2015**, *152*, 207–216. [[CrossRef](#)]
22. Velez, J.E.; Intrigliolo, D.S.; Castel, J.R. Scheduling deficit irrigation of citrus trees with maximum daily trunk shrinkage. *Agric. Water Manag.* **2007**, *90*, 197–204. [[CrossRef](#)]
23. Conejero, W.; Alarcon, J.J.; Garcia-Orellana, Y.; Abrisqueta, J.M.; Torrecillas, A. Daily sap flow and maximum daily trunk shrinkage measurements for diagnosing water stress in early maturing peach trees during the post-harvest period. *Tree Physiol.* **2007**, *27*, 81. [[CrossRef](#)] [[PubMed](#)]
24. Conejero, W.; Alarcón, J.J.; García-Orellana, Y.; Nicolás, E.; Torrecillas, A. Evaluation of sap flow and trunk diameter sensors for irrigation scheduling in early maturing peach trees. *Tree Physiol.* **2007**, *27*, 1753. [[CrossRef](#)]
25. Puerto, P.; Domingo, R.; Torres, R.; Pérez-Pastor, A.; García-Riquelme, M. Remote management of deficit irrigation in almond trees based on maximum daily trunk shrinkage. Water relations and yield. *Agric. Water Manag.* **2013**, *126*, 33–45. [[CrossRef](#)]
26. Du, S.; Tong, L.; Zhang, X.; Kang, S.; Du, T.; Li, S.; Ding, R. Signal intensity based on maximum daily stem shrinkage can reflect the water status of apple trees under alternate partial root-zone irrigation. *Agric. Water Manag.* **2017**, *190*, 21–30. [[CrossRef](#)]
27. Malheiro, A.C.; Pires, M.; Conceição, N.; Claro, A.M.; Dinis, L.-T.; Moutinho-Pereira, J. Linking Sap Flow and Trunk Diameter Measurements to Assess Water Dynamics of Touriga-Nacional Grapevines Trained in Cordon and Guyot Systems. *Agriculture* **2020**, *10*, 315. [[CrossRef](#)]
28. Li, D.; José, E.F.; Li, X.; Xi, B.; Jia, L.; Hernandez-Santana, V. Tree growth patterns and diagnosis of water status based on trunk diameter fluctuations in fast-growing *Populus tomentosa* plantations. *Agric. Water Manag.* **2020**, *241*, 106348. [[CrossRef](#)]
29. Carlos, M.; Carmina, R.; Amparo, M.; Gambetta, G.; Gravina, A.; Agustí, M. Tree water status influences fruit splitting in Citrus. *Sci. Hortic.* **2016**, *209*, 96–104.
30. Ruas, K.F.; Baroni, D.F.; de Souza, G.A.R.; de Paula Bernado, W.; Paixão, J.S.; dos Santos, G.M.; Machado Filho, J.A.; de Abreu, D.P.; de Sousa, E.F.; Rakocevic, M. A Carica papaya L. genotype with low leaf chlorophyll concentration copes successfully with soil water stress in the field. *Sci. Hortic.* **2022**, *293*, 110722. [[CrossRef](#)]
31. Zambrano-Vaca, C.; Zotarelli, L.; Beeson, R.C.; Morgan, K.T.; Migliaccio, K.W.; Chaparro, J.X.; Olmstead, M.A. Determining water requirements for young peach trees in a humid subtropical climate. *Agric. Water Manag.* **2020**, *233*, 106102. [[CrossRef](#)]
32. Wang, P. Study on the Integrated Development of Badam Industry in Shache County from the Perspective of Rural Revitalization. Master's Thesis, Tarim University, Alar, China, 2023.
33. Allen, R.G. Crop Evapotranspiration-Guidelines for computing crop water requirements. *FAO Irrig. Drain. Pap. (FAO)* **1998**, *56*, D05109.
34. Shi, Y.; Liu, Y.; Zhang, J. A study on the root distribution of peach trees. *J. Fruit Sci.* **1989**, *6*, 232–235.
35. Richards, A.L. Capillary conduction of liquids through porous mediums. *J. Appl. Phys.* **1931**, *1*, 318–333. [[CrossRef](#)]
36. Saray, G.; Iván, F.G.; Víctor, H.; Escalera, A.G.; Gil, F.F.; Amores-Agüera, J.J.; Rodríguez, B.C. Assessing the Water-Stress Baselines by Thermal Imaging for Irrigation Management in Almond Plantations under Water Scarcity Conditions. *Water* **2020**, *12*, 1298.
37. Gustavo, H.; Ferrarezi, R.S. Use of Thermal Imaging to Assess Water Status in Citrus Plants in Greenhouses. *Horticulturae* **2021**, *7*, 249.
38. Morandi, B.; Boselli, F.; Boini, A.; Manfrini, L.; Corelli, L. The fruit as a potential indicator of plant water status in apple. *Acta Hortic.* **2017**, *1*, 83–90. [[CrossRef](#)]
39. Girón, I.; Corell, M.; Martín-Palomo, M.; Galindo, A.; Torrecillas, A.; Moreno, F.; Moriana, A. Limitations and usefulness of maximum daily shrinkage (MDS) and trunk growth rate (TGR) indicators in the irrigation scheduling of table olive trees. *Agric. Water Manag.* **2016**, *164*, 38–45. [[CrossRef](#)]
40. Girón, I.F.; Corell, M.; Galindo, A.; Torrecillas, E.; Morales, D.; Dell'Amico, J.; Torrecillas, A.; Moreno, F.; Moriana, A. Changes in the physiological response between leaves and fruits during a moderate water stress in table olive trees. *Agric. Water Manag.* **2015**, *224*, 280–286. [[CrossRef](#)]

41. Sepulcre-Cantó, G.; Zarco-Tejada, P.J.; Jiménez-Muñoz, J.C.; Sobrino, J.A.; de Miguel, E.; Villalobos, F.J. Detection of water stress in an olive orchard with thermal remote sensing imagery. *Agric. For. Meteorol.* **2006**, *136*, 31–44. [[CrossRef](#)]
42. Corell, M.; Pérez-López, D.; Andreu, L.; Recena, R.; Centeno, A.; Galindo, A.; Moriana, A.; Martín-Palomo, M. Yield response of a mature hedgerow oil olive orchard to different levels of water stress during pit hardening. *Agric. Water Manag.* **2022**, *261*, 107374. [[CrossRef](#)]
43. Ru, C.; Hu, X.; Wang, W.; Ran, H.; Song, T.; Guo, Y. Evaluation of the Crop Water Stress Index as an Indicator for the Diagnosis of Grapevine Water Deficiency in Greenhouses. *Horticulturae* **2020**, *6*, 86. [[CrossRef](#)]
44. Li, S.H.; Jean-Gérard, H.; Bussi, C. Irrigation scheduling in a mature peach orchard using tensiometers and dendrometers. *Irrig. Drain. Syst.* **1989**, *3*, 1–12. [[CrossRef](#)]
45. Moller, M.; Alchanatis, V.; Cohen, Y.; Meron, M.; Tsipris, J.; Naor, A.; Ostrovsky, V.; Sprintsin, M.; Cohen, S. Use of thermal and visible imagery for estimating crop water status of irrigated grapevine. *J. Exp. Bot.* **2007**, *58*, 827. [[CrossRef](#)] [[PubMed](#)]
46. Drechsler, K.; Fulton, A.; Kisekka, I. Crop coefficients and water use of young almond orchards. *Irrig. Sci.* **2022**, *40*, 379–395. [[CrossRef](#)]
47. Yama, S.S.; Todorovic, M. Estimation of daily potato crop evapotranspiration using three different machine learning algorithms and four scenarios of available meteorological data. *Agric. Water Manag.* **2020**, *228*, 105875. [[CrossRef](#)]
48. Granata, F. Evapotranspiration evaluation models based on machine learning algorithms—A comparative study. *Agric. Water Manag.* **2019**, *217*, 303–315. [[CrossRef](#)]

**Disclaimer/Publisher’s Note:** The statements, opinions and data contained in all publications are solely those of the individual author(s) and contributor(s) and not of MDPI and/or the editor(s). MDPI and/or the editor(s) disclaim responsibility for any injury to people or property resulting from any ideas, methods, instructions or products referred to in the content.